Dansyl-β-cyclodextrins as Fluorescent Sensors Responsive to Organic Compounds

Yong WANG, Tsukasa IKEDA, Hiroshi IKEDA, Akihiko UENO,* and Fujio TODA
Department of Bioengineering, Faculty of Bioscience and Biotechnology, Tokyo Institute of Technology, 4259 Nagatsuta-cho, Midori-ku, Yokohama 227

(Received December 10, 1993)

6-O-, 2-O-, and 3-O-Dansyl-β-cyclodextrins (**1**, **2**, and **3**) were synthesized and characterized. Compounds **1** and **2** decrease their fluorescence intensities upon intermolecular complex formation. This property enables **1** and **2** to act as fluorescent sensors, converting binding of organic compounds into fluorescence variations.

Fluorescent sensors and chromogenic indicators that transform binding of molecules into spectroscopic signals are of current interest.[1,2] Some of these kinds of supramolecular systems are based on crown ethers, cryptands, and calixarenes with chromophores incorporated; such systems show absorption or fluorescence variations in response to inorganic cations upon host–guest complexation.[3—15] In those studies, absorption of fluorescence properties of the hosts were perturbed by a cation bound to the cavity of the macrocyclic part of the hosts. In contrast to the well-established sensory systems which are responsive to inorganic metal or ammonium cations, there have been few attempts to establish sensory systems which can transform binding of organic compounds into spectroscopic signals. Cyclodextrins (CDxs),[16,17] which are naturally existing oligosaccharides possessing a truncated shape and a central molecular cavity, can form inclusion (host–guest) complexes with a wide variety of organic species and might be used as the starting material for construction of sensory systems which are responsive to organic species. We have shown that modified CDxs with proper chromophores can be excellent systems to detect spectroscopically inert organic compounds by guest-induced spectroscopic changes that occur associated with formation of inclusion compounds.[2] Modified CDxs bearing fluorophores such as pyrene and naphthalene are examples of the sensors with which organic compounds are detected by variations in their emission spectra in aqueous solution.[18,19] They exhibit remarkable molecular recognition abilities for guest molecules. Circular dichroism spectra of modified CDxs may also be used, because the chromophore included in the chiral CDx cavities usually exhibits induced circular dichroism in the absorption region of the attached chromophore.[20]

In our CDx-based sensors, the spectroscopic signals are generated from the locational change of the chromophore(s) attached to CDx. This argument is implicated in the following structure features of the modified CDx and the nature of the chromophore. A fluorophore with adequate size attached to CDx as a pendant may form intramolecular complex by being included into the cavity of the CDx moiety. Upon guest addition, because of the binding of the guest, the modified CDx would exclude the fluorophore from inside to outside of the CDx cavity. This induced-fit guest binding thus results in a dramatic environmental change from the hydrophobic environment to the polar one around the fluorophore. If the emission of the fluorophore is sensitive to the microenvironment, the guest binding may lead to the desired guest-induced fluorescence variation.

Among fluorophores whose emissions are sensitive to the environment, dansyl (5-dimethylamino-1-naphthalenesulfonyl) probe is promising. Its fluorescence emission intensity is very sensitive to the polarity of the environment. In a polar solvent, such as water, its fluorescence emission is weak, but in nonpolar solvent it exhibits strong emission with a blue shift in fluorescence wavelength. It can be excited by light with a wavelength longer than 350 nm, where many organic compounds have no absorption, its Stokes shift is large, and its fluorescence is free from oxygen quenching, these details being important from practical points of view. Another important point of the probe is that the naphthalene ring is small enough to be included into the cavities of β, or γ-CDx.

The main entries to the CDx functionalization result from the selective reaction on the position C-6, C-2, or C-3 of the glucose moieties. We have found that γ-CDx can be selectively dansylated under different reaction conditions to provide mono 6-O-, 2-O-, or 3-O-substituted derivatives,[21] Using this synthetic method we prepared three kinds of dansyl-β-CDxs: 6-O-, 2-O-, and 3-O-dansyl-β-CDx (**1**, **2**, and **3**, respectively. Chart 1). The guest-induced fluorescence variations of **3** are rather complicated, and **3** seems to be unsuitable as the fluorescent sensor. Therefore, we report here mainly the guest-responsive behavior of **1** and **2**.

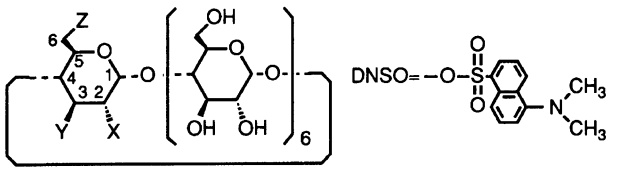

1: X = OH Y = OH Z = DNSO
2: X = DNSO Y = OH Z = OH
3: X = OH Y = DNSO Z = OH

Chart 1.

Results and Discussion

Syntheses and Structure Determinations of Monodansyl Modified β-CDxs. CDxs have the shape of truncated cone with the primary hydroxyls (C-6) on the narrower rim and the secondary hydroxyls (C-2 and C-3) on the wider rim. There are three possible positions for substitution in CDxs, C-6, C-2, and C-3, and we prepared all these members of dansyl-modified CDxs. The primary substituted β-CDx derivative **1** was prepared by the reaction of dansyl chloride and β-CDx in pyridine, employing a well-established means for preparation of primary substituted sulfonate of CDx.[22] The reaction proceeded successfully, with concomitant production of primary disubstituted dansyl CDx as side product. Compound **1** was separated from the unreacted CDx and disubstituted dansyl-CDxs through reversed-phase column chromatography. Its purity was confirmed by TLC, HPLC, and elemental analysis. The 500 MHz ^{1}H NMR spectrum of the sample gave 6 : 7 as the ratio of aromatic protons of the naphthalene moiety and the anomeric protons, the ratio being the expected one for monosubstituted derivatives. It could be converted to iodo derivative by the reaction with potassium iodide in DMF at 80 °C. It is known that the primary substituted 6-O-tosyl CDx can react with nucleophile to give replacement products,[22] while the secondary substituted tosylate is unreactive to nucleophilic replacement,[23] as expected from Richardson's rule.[24] So **1** is undoubtedly the 6-O-dansyl-β-CDx. More evidence comes from the comparison with the two authentic secondary monodansyl-β-CDx derivatives we prepared.

Sulfonation on the secondary side of CDx is more troublesome than that on the primary side, since the secondary hydroxyls are less reactive than the primary hydroxyls in organic solvents, and the secondary substituted products are unstable in alkaline solution due to the rapid conversion to epoxides. It is conceivable that the preparation of the secondary substituted sulfonyl CDx derivatives should be achieved by indirect ways,[23,25] or by protection of the primary hydroxyls.[26] But some reports of direct sulfonation on the secondary side of CDx using sulfonyl chloride were reported. Takahashi et al.[27] studied the reaction of CDx with tosyl chloride in aqueous sodium hydroxide solution, and found that with α-CDx, 2-O-tosyl-α-CDx was obtained, while with β-CDx, only 6-O-tosyl-β-CDx was produced. Fujita et al.[28] studied sulfonation of CDxs in alkaline aqueous solution with powdered sulfonyl chlorides, and found that sulfonation in the secondary side of CDxs can be achieved by the reaction of CDxs with sulfonyl chlorides in alkaline solution where pH of the reaction mixture was allowed to decrease as the reaction proceeds. According to this procedure the epoxide formation could be depressed. Although the secondary hydroxyls of CDx are less reactive than the primary ones in organic solution, since the acidity of secondary hydroxyls (pK_a 12.2) are much stronger than that of primary ones in water,[29] we think the secondary hydroxyls can be selectively sulfonated in water. However, since the solubility of the sulfonyl chloride used are very low in water, the actual reaction rate would be very slow. So the secondary substituted sulfonate can hardly be obtained due to the epoxidation. We solved this problem by using *N*,*N*-dimethylformamide (DMF) aqueous solution. When we poured the cyclodextrin solution of 0.25 M (1 M=1 mol dm^{-3}) pH 10.0 carbonate buffer into a vigorously stirred solution of dansyl chloride in DMF, we found that the dansyl chloride was consumed completely before it precipitated from the solution. The reaction was stopped by adding hydrochloric acid after a few seconds. Within this short period, epoxide formation from secondary substituted products actually did not occur. HPLC analysis indicates that almost no 6-O-dansyl-CDx was produced. But both 2-O- and 3-O-dansyl-CDxs, whose structures were determined later, were obtained with relatively high yields. When the dansyl chloride solution in DMF was poured into the CDx solution of water buffer, dansyl chloride precipitated from the solution instantaneously, resulting in a slow reaction, and the secondary dansyl-CDxs could not be obtained.

^{1}H NMR and elemental analysis show that **2** and **3** are monosubstituted dansyl-β-CDxs. Their purity was confirmed by TLC, HPLC, and elemental analyses. Both **2** and **3** are recovered unchanged from the KI reaction (80 °C, 2h in DMF). To determine their chemical structures, **2** and **3** were converted to their corresponding epoxides, **4** and **5**, respectively. The samples of **4** and **5** were free of aromatic protons in the 500-MHz ^{1}H NMR (D_2O) and showed one-proton singlet signal at $\delta=5.28$, and one-proton doublet signal at $\delta=5.31$ ($J_{12}=3.67$ Hz), respectively, for the anomeric proton of the glucose epoxide residue. This indicates that **4** and **5** were the manno-epoxide and allo-epoxide, respectively. So their predecessors, **2** and **3**, are undoubtedly dansyl-modified-β-CDxs substituted at the C-2 and C-3 positions, respectively.[28,30]

UV Absorption of 1 and 2 in the Absence and Presence of a Guest. Figures 1 and 2 show UV absorption spectra of **1** and **2**, respectively, without and with various concentrations of 1-adamantanol in pH 7.00 phosphate buffer. Dansyl group absorption has no fine structure and shows one broad band in the near-ultraviolet region. Compound **1** has a maximum absorption at 342.2 nm, while **2** has its peak at 335.0 nm. With host concentration kept constant, addition of increasing concentrations of 1-adamantanol brought about progressive blue shifts in the band maximum and increases in the absorption intensity. The guest-induced absorption change is larger for **1** than for **2**. Both **1** and **2** show the isosbestic point at 354.5 and 357.0 nm, respectively. Similar UV absorption variations were ob-

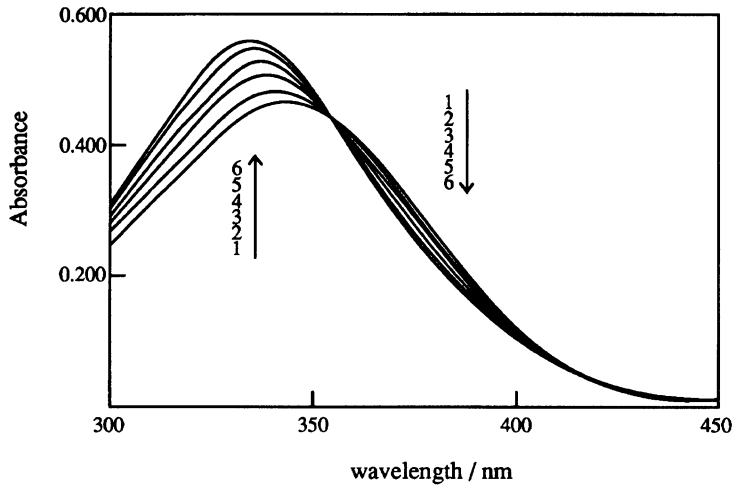

Fig. 1. UV absorption spectra of **1** in the absence and in the presence of various concentrations of 1-adamantanol. [**1**]=0.120 mM, 25 °C, pH=7.0, I=0.1 M. [1-adamantanol]: 1, 0; 2, 30 μM; 3, 60 μM; 4, 100 μM; 5, 200 μM; 6, 500 μM.

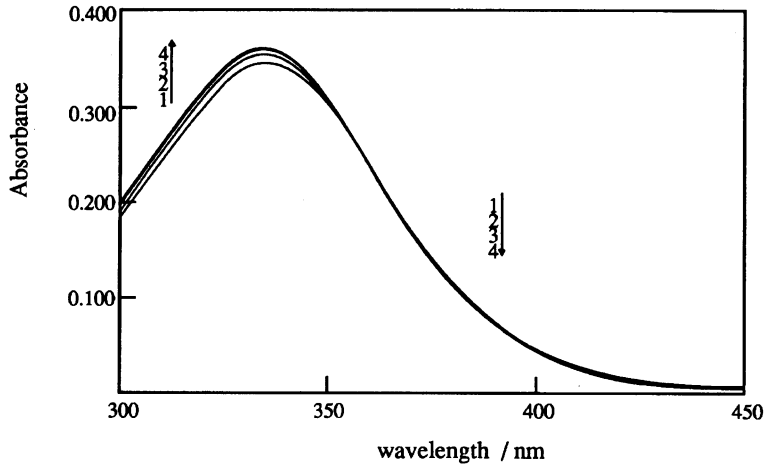

Fig. 2. UV absorption spectra of **2** in the absence and in the presence of various concentrations of 1-adamantanol. [**2**]=0.0700 mM, 25 °C, pH=7.0, I=0.1 M. [1-adamantanol]: 1, 0; 2, 50 μM; 3, 150 μM; 4, 1 mM.

served for the other guests illustrated in Chart 2, and the isosbestic points for them are the same as those for 1-adamantanol within experimental errors. The presence of the isosbestic points suggests that **1** or **2** is in equilibrium with the complex in which 1-adamantanol is included. The guest-induced UV absorption variation of **1** or **2** indicates that there are two distinct absorption spectra for free and complexed species for both **1** and **2**. This suggests that there occurs an environmental change around the dansyl group associated with guest binding.

Induced Circular Dichroism (ICD) Spectra of 1 and 2 in the Absence and Presence of a Guest. The CD spectra of **1** and **2** are shown in Figs. 3 and 4, respectively. Both **1** and **2** have a positive ICD band near 350 nm in water. But they displayed a different pattern of ICD bands near 250 nm, with a positive ICD band for **1** and a negative ICD band for **2**. Upon addition of 1-adamantanol (0.50 mM, according to the binding constants we obtained, at this concentration of

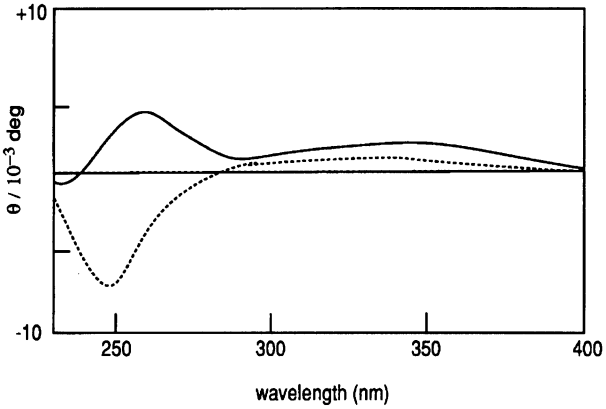

Fig. 3. CD spectra of **1** in the absence (——) and in the presence of 0.500 mM 1-adamantanol (- - -). [**1**]= 0.100 mM, 25 °C, pH=7.0, I=0.1 M.

1-adamantanol more than 90% of **1** and **2** were complexed), significant changes in the ICD spectra of **1** and **2** were observed. The positive ICD bands near 350 nm

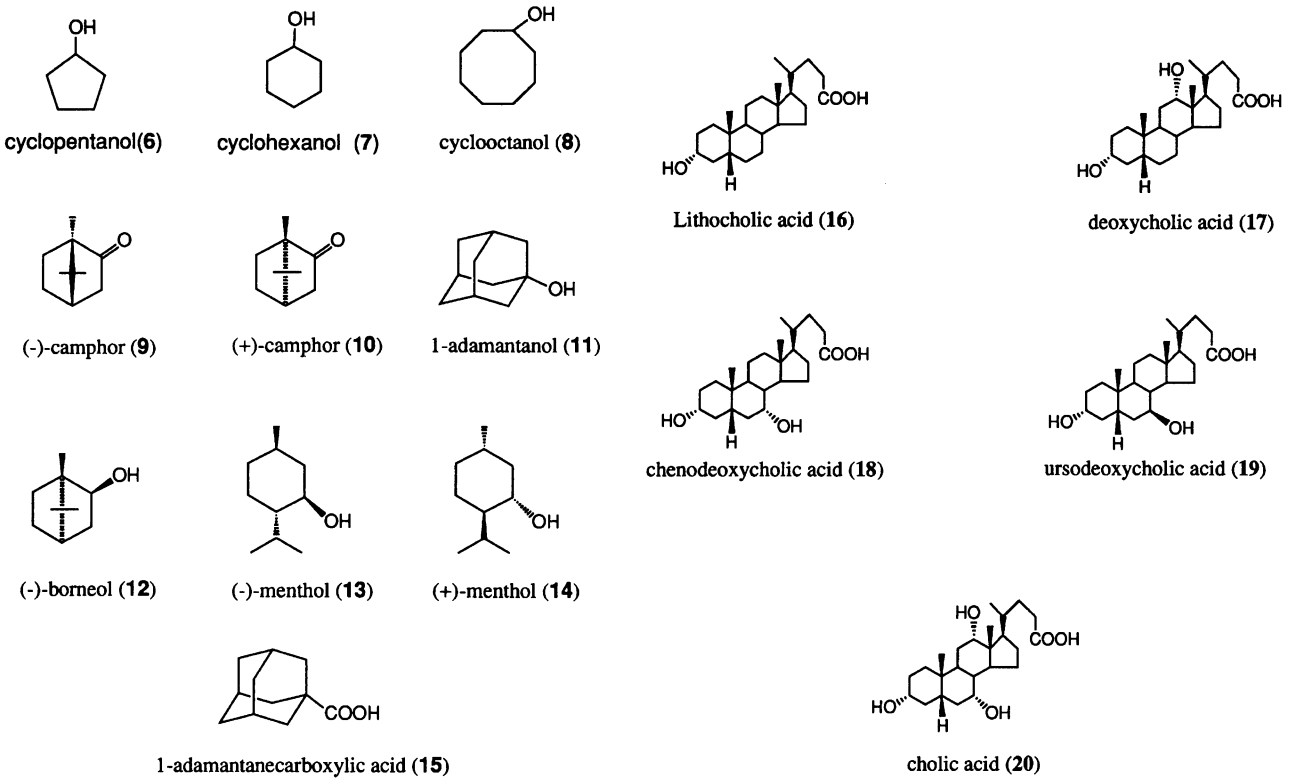

Chart 2.

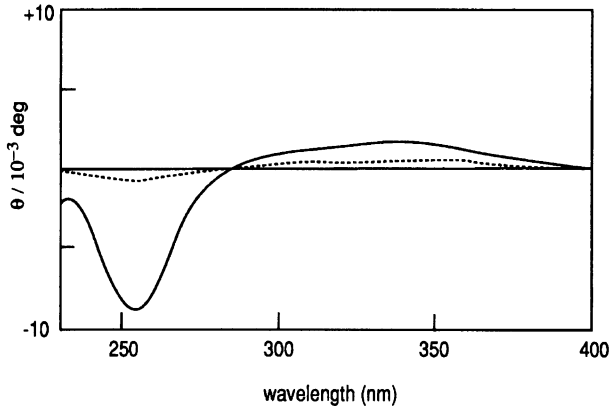

Fig. 4. CD spectra of **2** in the absence (—) and in the presence of 0.500 mM 1-adamantanol (---). [**2**]= 0.100 mM, 25 °C, pH=7.0, I=0.1 M.

for both **1** and **2** were depressed. The negative ICD band of **2** near 250 nm was also depressed. But the corresponding positive ICD band of **1** was reversed. Similar changes were observed for other guests we used. The significant spectral changes in the ICD absorption of both **1** and **2** were caused by the orientational and/or locational changes of the dansyl moiety of **1** and **2** upon guest binding. Although a quantitative analysis of ICD change is unavailable at the present stage because of lack of structural data of **1** or **2**, they are consistent with the suggestion that upon complex formation with guests the dansyl groups of **1** and **2** undergo locational changes in which the exclusion of dansyl group from the cavity of β-CDx seems to be the most possible way.

Fluorescence Emission of 1 and 2 in the Absence and Presence of a Guest. Figures 5 and 6 show fluorescence emission spectra of **1** and **2** respectively, in the absence and in the presence of various concentrations of 1-adamantanol. Spectra were excited at 354.5 nm for **1**, and 357.0 nm for **2**, which are isosbestic points of their UV absorption spectra shown in Figs. 1 and 2. It is well-known that the emission spectrum of dansyl group consists of one broad band without any fine structure. The spectra of **1** and **2** alone exhibit a peak at 570 and 548 nm, respectively. Upon addition of a guest, both **1** and **2** reduced fluorescence intensity with a red shift. This guest-induced variation in the fluorescence intensity is evidence for the fact that the dansyl group moves from the interior of the hydrophobic cavity toward the bulk water when **1** or **2** forms an intermolecular complex with a guest. This is reasonable since the dansyl moiety emits intensively in nonpolar solvent with short wavelength, while it emits weakly in polar solvent with a longer wavelength. This is also consistent with the fact that the fluorescence of dansylamine is enhanced when included by β-CDx.[31] The change of the emission intensity is much larger for **2** than for **1**. It is remarkable that more than 50 nm red shift of emission maximum for **2** is observed upon addition of 1 mM 1-adamantanol, while the change for **1** is almost negligible.

Lifetime Measurements. It is interesting to know

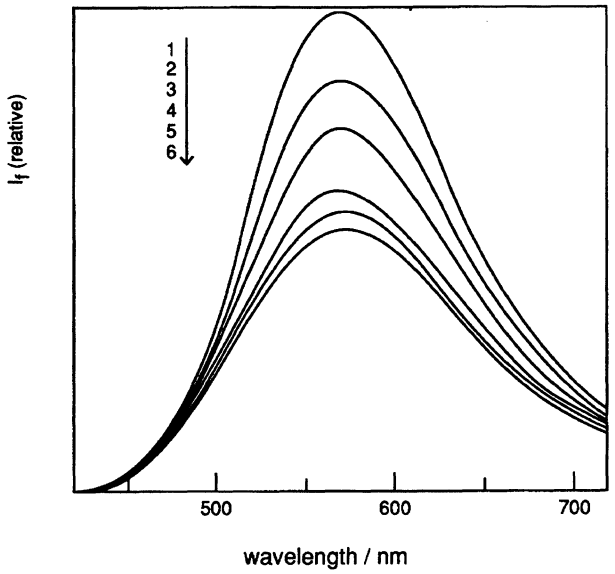

Fig. 5. Fluorescence emission spectra of **1** in water solution containing varying concentrations of 1-adamantanol. [**1**]=10 μM, 25 °C, pH=7.0, I=0.1 M. Excitation wavelength is 354.5 nm. [1-adamantanol]: 1, 0; 2, 20 μM; 3, 50 μM; 4, 150 μM; 5, 300 μM; 6, 1.00 mM.

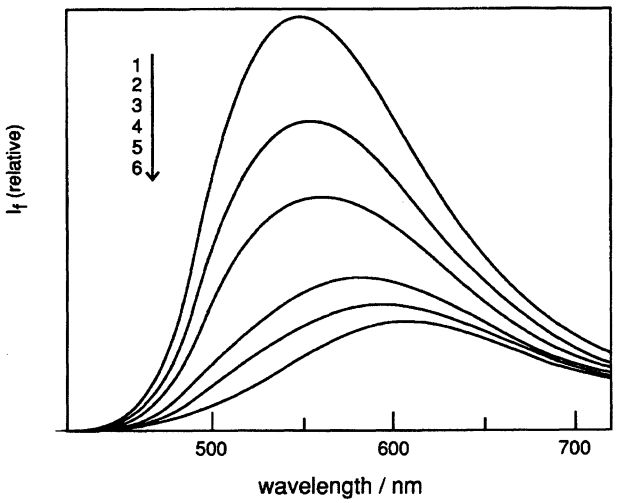

Fig. 6. Fluorescence emission spectra of **2** in water solution containing varying concentrations of 1-adamantanol. [**2**]=10 μM, 25 °C, pH=7.0, I=0.1 M. Excitation wavelength is 357.0 nm. [1-adamantanol]: 1, 0; 2, 20 μM; 3, 50 μM; 4, 150 μM; 5, 300 μM; 6, 1.00 mM.

more details about the guest-induced conformational change of **1** and **2**. The fluorescence lifetime of dansyl group can vary from hundreds of picoseconds to tens of nanoseconds depending on the solvent polarity. Thus fluorescence decay measurement would provide useful information about the environment around the dansyl groups of **1** and **2**.

The fluorescence decays of **1** or **2** could not be fitted to any single exponential function, but the curves were fitted well to a linear combination of two exponential functions. The results are summarized in Table 1. The existence of a shorter lifetime component and a longer one for both **1** and **2** in water solution indicates that the dansyl group is located in two different environments, a polar one and a less polar one. This is compelling evidence that **1** and **2** exist in two conformers, I and II, as illustrated in Fig. 7. In conformer I, the dansyl group is in a less polar environment because of being partially included in the β-CDx cavity, and corresponds to the longer lifetime component. In conformer II, the dansyl group is in a more polar environment because of being located outside the β-CDx cavity, and corresponds to the shorter lifetime component. The addition of 1-adamantanol into the aqueous solution of **1** or **2**, dramatically changes the relative emission quantum yields of the two lifetime components. The emission of the longer lifetime component is reduced, while the emission of the shorter one is enhanced. Obviously this indicates that there exists a dynamic equilibrium between the two conformers, which is driven to the shorter lifetime component side when the intermolecular complex is formed (Fig. 7).

Fluorescence of 3. In this article we concentrated our study mainly on **1** and **2**. The guest-induced fluorescence variation of **3** is very complicated. Here we wish to report some unusual fluorescence behavior of **3**. The aqueous solution of **3** has a typical emission spectrum of a dansyl group. But the emission maximum (520 nm) is shorter and emission intensity is much stronger than

Table 1. Fluorescence Lifetimes of **1** and **2**[a)]

	None		In the presence of 1-adamantanol[b)]	
	τ_1/ns (ϕ_1)	τ_2/ns (ϕ_2)	τ_1/ns (ϕ_1)	τ_2/ns (ϕ_2)
1	4.02 (0.740)	12.5 (0.260)	4.09 (0.802)	12.6 (0.198)
2	1.79 (0.106)	14.8 (0.894)	1.70 (0.691)	14.8 (0.309)

a) Decay curves were fitted to the equation: $I(t)=A_1\exp(-t/\tau_1)+A_2\exp(-t/\tau_2)$. Relative quantum yield was calculated by multiplying each lifetime and A-factor, and was normalized, $\phi_i=A_i\tau_i/(A_1\tau_1+A_2\tau_2)$. [**1**] = [**2**] = 20 μM, 25 °C, pH=7.0, I = 0.1 M. b) [1-adamantanol]=0.5 mM.

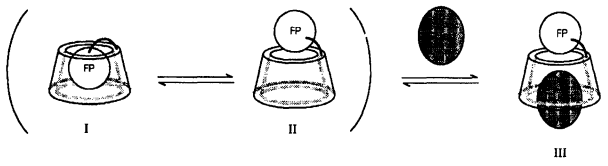

Fig. 7. Schematic illustration of the equilibrium between intramolecular and intermolecular inclusion complex. "FP" denotes the fluorescent probe.

those of **1** or **2**. Although its fluorescence decay could be analyzed by two lifetime components, the lifetimes, τ_1 17.1 ns (ϕ_1 0.930) and τ_2 40.1 ns (ϕ_2 0.070), contain no component arising from emission of the dansyl group in polar environment. The strong emission intensity, short emission maximum wavelength, and long emission lifetime indicate that in water solution the dansyl group of **3** is deeply and completely included into the β-CDx cavity. Addition of 1-adamantanol into an aqueous solution of **3** resulted in decrease of fluorescence intensity, but this process is very slow and is on a time scale of a few minutes. Figure 8 shows the time dependence of fluorescence change induced by 1-adamantanol. The rate of intermolecular complex formation between guest and **3** should be reflected in the rate of fluorescence decrease induced by the guest. It is known that CDxs form intermolecular inclusion complexes very fast, often with a rate constant larger than 10^9 $M^{-1}s^{-1}$. Thus the inclusion complex formation of **3** is abnormally slow. The examination of CPK molecular models suggests that when the dansyl group is deeply included into the β-CDx cavity, the excluding of dansyl group out from the β-CDx cavity would require a dramatic deformation of the β-CDx moiety. Thus the abnormality in the rate of intermolecular complex formation for **3** might be explained in terms of the high free energy of activation for this kind of structural deformation. Also we found that the fluorescence intensity of **3** as a function of concentration of guest could not be analyzed by 1:1 type Benesi–Hildbrand equation.

Sensory System. As described above, **1** and **2** decrease their fluorescence intensities associated with the formation of intermolecular inclusion complexes with 1-adamantanol. This property indicates that **1** and **2** may become sensory systems responsive to organic compounds. We selected a variety of organic compounds as guests to examine sensor abilities of **1** and **2**. They were given with numerical numbers in the order of increasing molecular weight (Chart 2). In order to illustrate the sensitivities of our sensory systems, we defined $\Delta I/I_0$, as the sensitivity factor, where $\Delta I = I_0 - I$, and I_0 and I stand for fluorescence intensity of **1** or **2** in the absence and in the presence of a guest, respectively.

The equilibrium shown in Fig. 7 can be written as

$$H(1) \rightleftharpoons H(2), \quad H(2) + G \rightleftharpoons HG$$

H(1) and H(2) are two conformers of **1** or **2**, G is the guest, and HG denotes the complex between guest and **1** or **2**. The macro binding constant K_b is defined as

$$K_b = [HG]/([H][G])$$

where $[H]=[H(1)]+[H(2)]$. Thus the nonlinear Benesi–Hildbrand equation for complex with 1:1 stoichiometry can be deduced as (see Appendix)

$$I = I_0 - a[HG]/[H]_0 \quad (1)$$

where,

$$[HG] = ([H]_0 + [G]_0 + K_b^{-1} - (([H]_0 + [G]_0 + K_b^{-1})^2 - 4[H]_0[G]_0)^{0.5})/2 \quad (2)$$

$[H]_0$ and $[G]_0$ are the total concentrations of **1** (or **2**) and guest, respectively, a is an experimental constant representing the difference between the fluorescence intensity in the absence of guests and that in the presence of an infinite concentration of guests.

In many cases (expect for $K_b > 10^4$ M^{-1}), where $[G]_0 \gg [H]_0$, Eq. 2 can be simplified as

$$[HG] = [H]_0[G]_0/\left([H]_0 + [G]_0 + K_b^{-1}\right) \quad (3)$$

In our measurements, we kept the host concentration at constant (10 μM) and measured the fluorescence changes induced by the guest at a fixed wave-

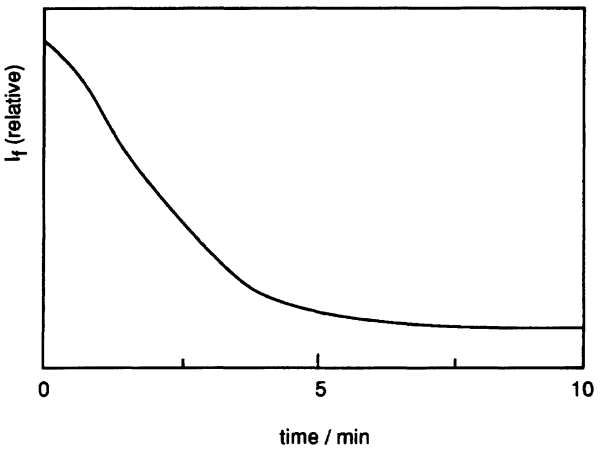

Fig. 8. Time-dependent fluorescence change of **3** after addition of 0.1 mM 1-adamantanol. [**3**]=5 μM, 25 °C, pH=7.0, I=0.1 M. Excitation and emission wavelengths are 340 and 500 nm, respectively.

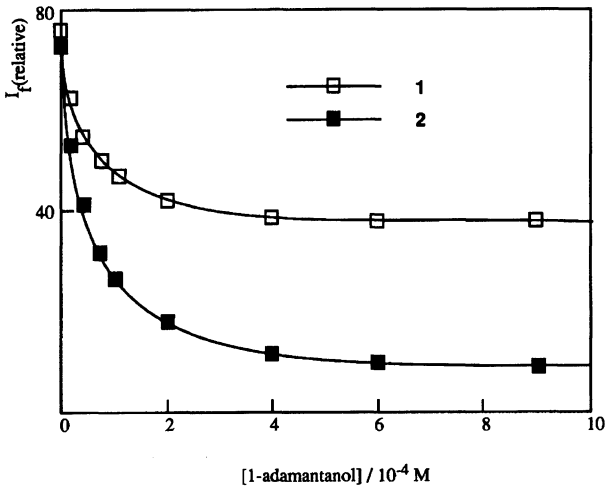

Fig. 9. Fluorescence titrations of **1** and **2** at 25 °C, as a function of 1-adamantanol concentration. The solid lines are calculated curves obtained by using Eq. 1.

Table 2. Binding Constants and Sensitivity Factors of **1** and **2** in Aqueous Solution[a)]

Guests	Hosts					
	1[b)]			**2**[c)]		
	$\Delta I/I_0$[d)]	$K_b \times 10^{-3}$ (M^{-1})	$(\Delta I/I_0)_{max}$	$\Delta I/I_0$[d)]	$K_b \times 10^{-3}$ (M^{-1})	$(\Delta I/I_0)_{max}$
6	0.005	0.109	0.503	0.011	0.130	0.807
7	0.038	1.04	0.509	0.041	0.582	0.841
8	0.151	4.35	0.510	0.222	3.71	0.836
9	0.163	3.95	0.562	0.295	5.38	0.884
10	0.148	3.77	0.557	0.311	5.34	0.885
11	0.390	31.4	0.527	0.636	24.9	0.911
12	0.320	18.5	0.506	0.537	16.0	0.878
13	0.196	6.61	0.525	0.248	4.06	0.846
14	0.185	6.07	0.518	0.230	3.47	0.860
15	0.375	37.6	0.494	0.650	28.1	0.902
16	0.608[e)]	5740	0.667	0.824[e)]	3934	0.864
17	0.125	2.76	0.531	0.311	6.29	0.803
18	0.537	64.8	0.629	0.782	155	0.849
19	0.609	1651	0.613	0.855	1050	0.864
20	0.075	1.30	0.545	0.193	2.92	0.796

a) Measured at 25 °C, pH=7.0, I=0.1 M, [**1**]=[**2**]=10 μM. b) Excitation and emission wavelengths were 345.5 and 560 nm, respectively. c) Excitation and emission wavelengths were 357.0 and 540 nm, respectively. d) [G]=0.100 mM. e) [**16**]=25.5 μM.

length. Computer simulation using fluorescence intensity as a function of guest concentration fitted Eq. 1 very well. Fluorescence titration and computer simulation for complex formation of 1-adamantanol with **1** and **2** are shown in Fig. 9. This is strong evidence for the 1 : 1 stoichiometry of the intermolecular complexation between **1** or **2** with the guests. This is reasonable, because under our measurement conditions the concentration of host is low enough to prevent formation of higher order complexes. Binding constants of **1** and **2** are summarized in Table 2.

Table 2 indicates that **1** and **2** have similar binding behavior for each guest. Binding constants of cyclopentanol (**6**) are very small due to its rather small size. Binding constants for cyclohexanol (**7**), cyclooctanol (**8**), camphor (**9**, **10**) and menthol (**13**, **14**), are slightly larger. The discrimination of each host for stereoisomers of camphor and menthol is detectable, but the degrees are small. Binding constants for 1-adamantanol (**11**), (−)-borneol (**12**), and 1-adamantanecarboxylic acid (**15**) are very high. This is because these ball-like molecules can be tightly bound to the β-CDx cavity. Lithocholic acid (**16**) is bound by **1** and **2** with tremendously high binding constants, on the order of 10^6 M^{-1}. This may be due to its high hydrophobicity which enables it to be tightly-fitted to the β-CDx cavity. The hydrophobic interaction between this guest and the DNS moiety may also contribute to this strong binding. Ursodeoxycholic acid (**19**) has one more hydroxyl group in its structure than **16** does, and its binding constants are smaller than those of **16**. Chenodeoxycholic acid (**18**) is an epimer of **19**. However, its binding constants are only about 1/25 for **1** and about 1/7 for **2** compared with those of **19**. Deoxycholic acid (**17**) is another isomer with one of the hydroxyl groups in a different position from that of **18** and **19**. This displacement results in a dramatic decrease of its binding constant for **1** as well as **2**. Cholic acid (**20**) has one more hydroxyl group in its structure, and exhibits the smallest binding constants among the stereoides.

The maximum sensitivity factor represents the sensitivity factor in the presence of an infinite concentration of guest. It can be calculated from the following equation:

$$(\Delta I/I_0)_{max} = a/I_0 \quad (4)$$

The values of $(\Delta I/I_0)_{max}$ are summarized in Table 2. It is clear that the $(\Delta I/I_0)_{max}$ are always larger for **2** than for **1**. The $(\Delta I/I_0)_{max}$ of **1** or **2** for various guests are different from each other, but the differences are small. This indicates that, although in the intermolecular complex state the dansyl group emits in different quantum yields for different guests, the emission is determined mainly by the polarity of the environment around the dansyl group. The sensitivity factor at any given guest concentration can be expressed as

$$\Delta I/I_0 = (\Delta I/I_0)_{max}[HG]/[H]_0 \quad (5)$$

Since $(\Delta I/I_0)_{max}$ is not much different from each other for different guests, the $\Delta I/I_0$ is mainly determined by [HG], that is, by the binding constants. Table 2 lists the sensitivity factor $\Delta I/I_0$ for various guests at the concentration of 0.100 mM. We can see that the values of $\Delta I/I_0$ are in consistent with the binding constants. Also, **2** is more sensitive than **1** to each of the guests due to its larger $(\Delta I/I_0)_{max}$ values.

Our results demonstrated that **1** and **2** do act as effective fluorescent sensors of molecular recognition for

converting binding of organic compounds into fluorescence variation. There exists a dynamic equilibrium between two conformers of **1** or **2**. The dansyl group of **1** and **2** is excluded from the inside of the cavity to outside when intermolecular complex is formed. Our model for the sensory mechanism is proposed on the basis of UV, ICD, steady fluorescence, and fluorescence lifetime measurements. The binding constants of our sensory systems for various guests differ from 1×10^2 to 5×10^6 M^{-1}, leading a good selectivity of our systems for a variety of organic compounds. The dansyl group of **3** is deeply and completely included into the cavity of the β-CDx moiety. This leads to its very complicated guest-induced fluorescence variation behavior.

Experimental

Materials and Methods. All guest molecules examined and dansyl chloride were purchased from Tokyo Kasei, and were used without further purification. Pyridine and *N*,*N*-dimethylformamide (DMF) were bought from Kanto Kagaku. Pyridine was dried with a molecular sieve for several days before use.

HP-20 resin (high porous polystyrene resin) was purchased from Mitsubishi Kasei. The methanol aqueous solution used as elution solvent is degassed by ultrasonic waves before use.

Thin-layer chromatography (TLC) was performed on Kieselgel 60 F_{254} (Merck) silica plate, using the mixed solvent of 1-buthanol : ethanol : water = 5 : 4 : 3. Compounds were visualized by UV irradiation and by spraying the plate with 5% sulfuric acid ethanol solution containing 5% *p*-anisaldehyde.

TSKgel ODS-80TM column (4.6×150 mm) and TSKgel ODS-120T (21.5×300 mm) were used for HPLC analysis and preparation, respectively. The flow rates for HPLC analysis and preparation were 0.5 and 4 ml min^{-1}, respectively. 30% methanol was used as solvent for HPLC analysis. Compounds were detected by a UV-detector, the wavelength being 340 nm.

UV absorption, steady fluorescence, and fluorescence decay measurements were performed in 0.1 M pH 7.00 phosphate buffer at 25 °C. Spectrometric grade water from Merck was used. UV absorption spectra were recorded on a Shimadzu UV-310 spectrophotometer. CD spectra were recorded on a JASCO J-600 spectropolarimeter. Fluorescence measurements were done on a Hitachi 850 fluorescence spectrophotometer. The excitation wavelength was 345.5 nm for **1** and 357.0 nm for **2**. The band width for both excitation and emission sides was 5.0 nm. Lifetime measurement were performed on a Horiba NAES-550 single photon counting nanosecond fluorometer. On the excitation side, a combination of filters (Hoya UV34, Hoya UV340, and Hoya 350) was used to obtain excitation light with wavelengths of 320—380 nm. On the emission side, a combination of filters (Hoya L42, Toshiba Y46, and $NiSO_4\cdot6H_2O$ 500 g dm^{-3}) was used to obtain the emission light with wavelengths of about 400—600 nm. At least 10^4 counts of maximum count were collected for each measurement. All instruments were equipped with a thermostat to keep the temperature at 25 °C with an accuracy of ±0.01 °C.

^{1}H NMR was measured on a Varian VXR-500S NMR instrument. D_2O and DMSO-d_6 from Merck were used. The residual proton absorptions of the deuterated solvents were used as the internal standards.

Synthesis of 1. To 200 ml of pyridine at room temperature was added 10 g β-CD, which was dried in advance for 24 h at 80 °C in vacuum. When the β-CD was dissolved, 1 g dansyl chloride was added. After about ten minutes the reaction mixture was analyzed by TLC. The R_f is 0.34 for β-CDx, 0.54 for monodansyl-β-CDx, and 0.78 for disubstituted dansyl-β-CDx. Another amount of dansyl chloride was added to obtain the maximum yield of monodansyl-β-CDx. Since the amount of dansyl chloride added was dependent on the water contained in pyridine and β-CDx, the amount was determined by TLC analysis of the reaction mixture. The reaction mixture thus obtained was concentrated to about 50 ml in vacuum, and then 1 liter acetone was added to precipitate β-CDx and its derivatives. The crude product was collected, dried in vacuum at room temperature overnight, then dissolved in 500 ml water. After filtration the solution was subjected to a HP-20 column (4×20 cm), which had been washed with methanol first, and then with water before use. The column was eluted in steps, with 10, 20, and 30% methanol aqueous solutions. The subsequent elution by 50—60% aqueous methanol gave the desired **1**. No disubstituted dansyl-β-CDx was eluted out at these methanol aqueous solutions. The elute was concentrated through evaporation in vacuum, and lyophilized to provide yellowish powder (6.5 g, yield 65%). R_f=0.54. HPLC retention time 14.0 min. Found: C, 45.16; H, 6.11; N, 0.93; S, 2.18%. Calcd for $C_{54}H_{81}NO_{37}S\cdot4H_2O$: C, 45.03; H, 6.23; N, 0.97; S, 2.23%. ^{1}H NMR (D_2O) (aromatic moiety) δ=8.83 (1H, d), 8.35 (1H, d), 8.12 (1H, d), 7.93 (1H, t), 7.63 (1H, t), 7.60 (1H, d); (anomeric protons) δ=5.09 (1H, d), 5.04 (1H, d), 5.01 (1H, d), 4.99 (1H, d), 4.93 (1H, d), 4.83 (1H, d), 4.80 (1H, d); $-N(CH_3)_2$, δ=2.90 (6H, s); other protons of CDx moiety, δ=3.0—4.4.

Syntheses of 2 and 3. Into a vigorously stirred DMF solution of dansyl chloride (1 g in 10 ml DMF) was poured 20 ml of 0.30 M pH 10.0 $NaHCO_3$–Na_2CO_3 buffer containing 3 g β-CDx (dissolved in small amount of DMF). After a few seconds, the reaction was stopped by adding hydrochloric acid to make the pH of the reaction mixture around 5. Then the mixture was concentrated almost to dryness under reduced pressure. The crude product was dissolved in 1 liter of water and this mixture was put into a HP-20 column (4×20 cm). According to the same procedure as described for **1**, the monodansyl-β-CDx was separated, collected, and lyophilized to provide a yellowish powder (2 g, yield 60%). Although this product exhibits single spot in TLC analysis (R_f 0.54), in reversed-phase chromatography it can be separated into two components, which were later identified as 2-O- and 3-O-dansyl-β-CDx, with retention time 9.0 min for **2**, 11.4 min for **3**. 500 mg of this products was dissolved in aqueous DMF; this mixture was injected into the HPLC column and eluted with 15% methanol–water to yield pure **2** (350 mg), and **3** (80 mg). For **2**, Found: C, 45.48; H, 6.32; N, 0.96; S, 2.31%. Calcd for $C_{54}H_{81}NO_{37}S\cdot3H_2O$: C, 45.60; H, 6.17; N, 0.98; S, 2.25%. ^{1}H NMR (DMSO-d_6) (aromatic protons) δ=8.52 (1H, d), 8.22 (2H, d), 7.64 (1H, t), 7.59 (1H, t), 7.25 (1H, d); anomeric protons δ=4.96 (1H, d), 4.83 (1H, d), 4.78 (4H, m), 4.74 (1H, d); $-N(CH_3)_2$, δ=2.82

(6H, s); other protons of CDx moiety, δ=3.10—4.40. For **3**, Found: C, 44.59; H, 6.30; N, 0.99; S, 2.18%. Calcd for $C_{54}H_{81}NO_{37}S\cdot 5H_2O$: C, 44.47; H, 6.29; N, 0.96; S, 2.20%. ^{1}H NMR (DMSO-d_6) (aromatic protons) δ=8.50 (1H, d), 8.23 (1H, d), 8.16 (1H, d), 7.63 (2H, t), 7.26 (1H, d); (anomeric protons) δ=4.99 (1H, d), 4.90 (1H, d), 4.81 (5H, m); $-N(CH_3)_2$, δ=2.87 (6H, s); other protons of CDx moiety, δ=3.15—4.42.

Epoxidation of 2 and 3. Compound **2** or **3** (100 mg each) was added into 20 ml 0.5% K_2CO_3 water solution. DMF was added drop by drop until the sample of **2** or **3** was dissolved. After 1 h TLC analysis indicated that **2** or **3** had converted into the epoxide completely (R_f=0.36 for epoxides). Dilute hydrochloric acid was added to put pH of the solution around 4, and then concentrated, filtrated and injected to HPLC equipped with ODS column. Washing with pure water and then 3% methanol–water gave the desired epoxide; **4** or **5**. For **4**, Found: C, 42.51; H, 6.37%. Calcd for $C_{42}H_{68}O_{34}\cdot 4H_2O$: C, 42.43; H, 6.44%. ^{1}H NMR (anomeric protons) δ=5.28 (1H, s), 5.14 (1H, d), 5.09 (5H, m); other protons, δ=3.50 (1H, d, J=3.85 Hz), 3.74—4.00 (majority, m). For **5**, Found: C, 43.19; H, 6.50%. Calcd for $C_{42}H_{68}O_{34}\cdot 3H_2O$: C, 43.08; H, 6.37%. ^{1}H NMR (anomeric protons) δ=5.31 (1H, d, J=3.67 Hz), 5.11 (6H, m), other protons, 3.74—4.00.

Appendix

Letting ε_1, ε_2, and ε_3 be the fluorescence intensities of H(1), H(2), and HG, respectively, at unit concentration, the fluororescence intensity of our sensory systems is

$$I = \varepsilon_1[\mathrm{H(1)}] + \varepsilon_2[\mathrm{H(2)}] + \varepsilon_3[\mathrm{HG}] \quad (6)$$

In the absence of a guest, we have:

$$I_0 = \varepsilon_1[\mathrm{H(1)}]_0 + \varepsilon_2[\mathrm{H(2)}]_0 \quad (7)$$

and

$$[\mathrm{H(1)}] + [\mathrm{H(2)}] + [\mathrm{HG}] = [\mathrm{H(1)}]_0 + [\mathrm{H(2)}]_0 \quad (8)$$

Putting:

$$[\mathrm{H(1)}] = [\mathrm{H(1)}]_0 - x \quad (9)$$

Then:

$$[\mathrm{H(2)}] = [\mathrm{H(2)}]_0 + x - [\mathrm{HG}] \quad (10)$$

From (6), (7), (9) and (10):

$$I = I_0 + (\varepsilon_2 - \varepsilon_1)\, x + (\varepsilon_3 - \varepsilon_2)\,[\mathrm{HG}] \quad (11)$$

Letting k be the equilibrium constant between H(1) and H(2):

$$k = [\mathrm{H(2)}]/[\mathrm{H(1)}] = [\mathrm{H(2)}]_0/[\mathrm{H(1)}]_0 \quad (12)$$

From (9), (10), and (12):

$$x = [\mathrm{HG}]/(1+k) \quad (13)$$

From (11) and (13):

$$I = I_0 + ((\varepsilon_2 - \varepsilon_1)/(1+k) + \varepsilon_3 - \varepsilon_2)\,[\mathrm{HG}] \quad (14)$$

Putting:

$$a = -((\varepsilon_2 - \varepsilon_1)/(1+k) + \varepsilon_3 - \varepsilon_2)\,[\mathrm{H}]_0 \quad (15)$$

Combining (14) and (15):

$$I = I_0 - a[\mathrm{HG}]/[\mathrm{H}]_0 \quad (1)$$

References

1) A. W. Czarnik, in "Frontiers in Supramolecular Organic Chemistry and Photochemistry," VCH, Weinheim (1991), pp. 109—122.

2) A. Ueno and T. Osa, in "Photochemistry in Organized and Constrained Media," VCH, New York (1991), pp. 739—782.

3) H.-G. Lohr and F. Vogtle, *Acc. Chem. Res.*, **18**, 65 (1985).

4) U. Herrmann, B. Tummlar, G. Maass, P. K. T. Mew, and F. Vogtle, *Biochemistry*, **23**, 4059 (1984).

5) J. P. Konopelski, F. Kotzyba-Hilbeert, J.-M. Lehn, J.-P. Desvergne, F. Fagas, A. Castellan, and H. Bouas-Laurent, *J. Chem. Soc., Chem. Commun.*, **1985**, 433.

6) H. Bounas-Laurent, A. Castellan, M. Danay, J.-P. Desvergne, G. Guinand, P. Marsan, and M.-H. Riffand, *J. Am. Chem. Soc.*, **108**, 315 (1986).

7) F. Fagas, J.-P. Desvergne, H. Bounas-Laurent, P. Marsan, F. A. Kotzyba-Hilbeert, and M. Joubbeh, *J. Am. Chem. Soc.*, **111**, 8672 (1989).

8) F. Fagas, J.-P. Desvergne, H. Bounas-Laurent, J.-M. Lehn, J. P. Konopelski, P. Marsan, and M.-H. Riffand, *J. Chem. Soc., Chem. Commun.*, **1990**, 655.

9) S. Ogawa, R. Naruhashi, and Y. Arai, *J. Am. Chem. Soc.*, **106**, 5760 (1984).

10) H. Shizuka, K. Takeda, and T. Morita, *J. Phys. Chem.*, **84**, 994 (1980).

11) O. S. Wolfbeis and H. Offenbacher, *Monatsh. Chem.*, **115**, 647 (1984).

12) R. C. Helgeson, B. P. Czech, E. Chapoteau, C. R. Gebauer, A. Kumar, and D. J. Cram, *J. Am. Chem. Soc.*, **111**, 6339 (1989).

13) F. U. Akkaya, M. E. Huston, and A. W. Czarnik, *J. Am. Chem. Soc.*, **112**, 3590 (1989).

14) I. Aoki, H. Kawabata, K. Nakashima, and S. Shinkai, *J. Chem. Soc., Chem. Commun.*, **1991**, 1771.

15) I. Aoki, T. Sakaki, and S. Shinkai, *J. Chem. Soc., Chem. Commun.*, **1992**, 730.

16) M. I. Bender and M. Komiyama, "Cyclodextrin Chemistry," Springer-Verlag, New York (1977).

17) J. Szejtli, "Cyclodextrin and Their Inclusion Complexes," Akademiai Kiado, Budapast (1982).

18) A. Ueno, I. Suzuki, and T. Osa, *Anal. Chem.*, **62**, 2461 (1990).

19) A. Ueno, S. Minato, and T. Osa, *Anal. Chem.*, **64**, 2562 (1992).

20) A. Ueno, Q. Chen, and T. Osa, *Anal. Chem.*, **64**, 1650 (1992).

21) Y. Wang, T. Ikeda, A. Ueno, and F. Toda, *Chem. Lett.*, **1992**, 863.

22) L. D. Melton and K. N. Slessor, *Carbohydr. Res.*, **18**, 29 (1971).

23) A. Ueno and R. Breslow, *Tetrahedron Lett.*, **23**, 3451 (1982).

24) A. C. Richardson, *Carbohydr. Res.*, **10**, 395 (1969).

25) T. Murakami, K. Harata, and S. Morimoto, *Tetrahedron Lett.*, **28**, 321 (1987).

26) M. J. Pregel and E. Buncel, *Can. J. Chem.*, **69**, 130

(1991).
27) K. Takahashi, K. Hattori, and F. Toda, *Tetrahedron Lett.*, **25**, 3331 (1984).
28) K. Fujita, S. Nakamura, and T. Imoto, *Tetrahedron Lett.*, **25**, 5673 (1984).
29) T.-F. Chin, P.-H. Chung, and J. L. Lach, *J. Pharm. Sci.*, **44**, 57 (1968).
30) R. Breslow and A. W. Czarnik, *J. Am. Chem. Soc.*, **105**, 1390 (1983).
31) G. C. Catena and F. V. Bright, *Anal. Chem.*, **61**, 905 (1989).